Tin Oxide Nanooctahedra

Self-Construction of Hollow SnO_2 Octahedra Based on Two-Dimensional Aggregation of Nanocrystallites**

*Hua Gui Yang and Hua Chun Zeng**

The past few years have witnessed an increasing trend toward synthetic fabrication of micro- and nanostructures with hollow interiors, owing to their potential applications as photonic crystals, host materials for intercalants, drug-delivery carriers, sensors, and chemical reactors.[1–14] These hollow structures, which normally consist of inorganic materials such as metals or metal oxides, provide both chemical functionality and designable inner space for meeting new technological challenges. Among many preparative methods,[1–14] template-assisted synthesis is an effective approach in which hard templates, such as polymeric core supports or sacrificial metal substrates, and soft templates, such as micelles in emulsions or ionic liquids, have been utilized.[1–11] Recent developments in this area show that hollow structures can also be created via direct solid evacuation with Ostwald ripening,[12] and the Kirkendall effect,[13] or formed from self-assembly of building blocks through hydrophobic interactions.[14] It would also be desirable to search for one-pot syntheses, preferably by template-free routes.

"Oriented attachment" has attracted increasing interest in recent years as a new means for fabrication and self-organization of nanocrystalline materials under one-pot conditions.[15–19] As summarized in Figure 1, recent examples include formation of one-dimensional (1D) nanorods (e.g., TiO_2 and ZnO) from their respective 0D nanocrystallites (Figure 1a).[15,16] The formed 1D nanorods or nanoribbons can also further self-attach through stacking by planar van der Waals interaction (for layered compounds, e.g., α-MoO_3; Figure 1b)[17] or lateral "lattice fusion" (for ionic compounds, e.g., ZnO; Figure 1c)[16,18] to generate either length-multiplied 1D nanostructures or 2D crystal sheets and walls. Recently, this size-amplifying mechanism was extended to 3D architectures of 2D crystal strips (formed from 1D nanoribbons; Figure 1d),[19] in which rhomb-shaped 2D building blocks can self-aggregate into "dandelion"-like hollow spheres. Here we report another novel organizing principle (Figure 1e) with an underlying oriented-attachment mechanism in which complex geometrical structures (e.g., polyhedra) can be built by the assembly route 0D→2D→3D. Using the wide-band-gap semiconductor tin dioxide as an example,[11,20,21] we demonstrate that hollow geometrical

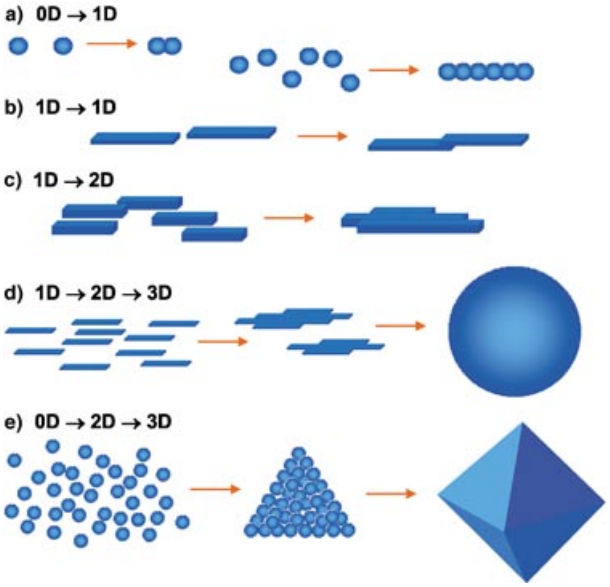

Figure 1. Various organizing schemes for self-construction of nanostructures by oriented attachment.

[*] H. G. Yang, Prof. Dr. H. C. Zeng
Department of Chemical and Biomolecular Engineering
Faculty of Engineering
National University of Singapore
10 Kent Ridge Crescent, Singapore 119260 (Singapore)
Fax: (+65) 6779-1936
E-mail: chezhc@nus.edu.sg

[**] The authors gratefully acknowledge the financial support of the Ministry of Education, Singapore.

Supporting information for this article is available on the WWW under http://www.angewandte.org or from the author.

  DOI: 10.1002/ange.200461129

objects of micro- and nanoscales can be prepared by one-pot solution routes without using templates. This strategy is based on the ability to stabilize certain crystallographic planes while the 0D nanocrystallites form and undergo 2D self-aggregation.

The crystallographic structure and chemical composition of the SnO_2 octahedra were determined by powder XRD and energy-dispersive X-ray spectroscopy (EDX; Supporting Information). These data show that the prepared SnO_2 has a rutile-like tetragonal symmetry and a strictly stoichiometric atomic ratio (space group $P4_2/mnm$, $a_o = 4.738$, $c_o = 3.188$ Å; JCPDS file no. 21-1250;[11,20,21] Sn/O = 1:2). In particular, the broad XRD peaks of (110), (101), (200), (211), and (112) reflect the nanocrystalline nature of samples, but no lattice relaxation was detected.

The field-emission scanning electron microscopy (FESEM) images in Figure 2a show the general morphology of the hollow SnO_2 octahedra synthesized in this work. A high yield (> 95 %) of this polyhedral form can be easily achieved after only one sedimentation run (Figure 2e). Interestingly,

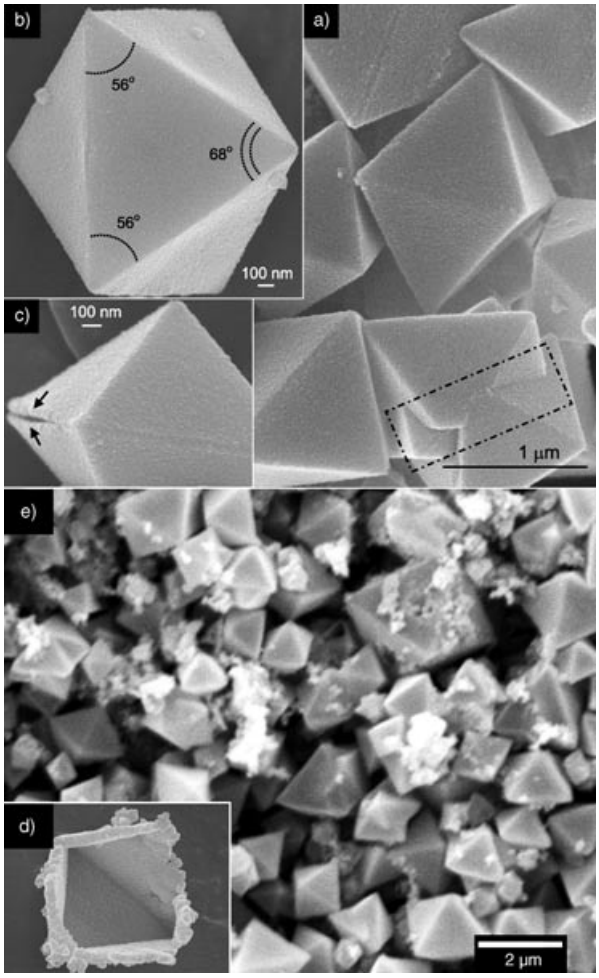

Figure 2. FESEM images of hollow SnO_2 crystal octahedra. a) General sample morphology (the framed area indicates the joined part of two intersecting octahedra). b) A tilted SnO_2 octahedron. c) Ridge opening (indicated by arrows) on a SnO_2 octahedron. d) Interior morphology. e) Overall product morphology after only one sedimentation run (SEM image).

geometrical parameters of the bipyramidal octahedra, such as interplanar angles and edge-length ratios, are essentially identical regardless of the actual sizes of the hollow structures (Supporting Information). This observation indicates that an overall crystallographic relationship exists among the nanocrystallites that constitute the octahedra. The isosceles-triangular crystal planes (Figure 2b) have angles of 56 ± 1 and $68 \pm 1°$,[22] that is, the crystallographic planes of each octahedral surface are similar to the {111} family (Figure 3d). There is a total of 16 {111}-like planes per octahedron: eight for inner surfaces, and eight for outer ones. The interior space of the hollow SnO_2 octahedra was examined directly by FESEM for incomplete or cracked SnO_2 crystal octahedra (Figure 2d). The size of these hollow octahedra can be as small as 150 nm to as large as several micrometers (Figure 2e), and the thickness of the shell walls is in the range of 20–200 nm, depending on synthetic conditions (see also Supporting Information). In general, higher initial concentrations of SnF_2 and longer reaction times lead to the formation of larger octahedra.

The hollow interior and geometrical symmetry of the as-synthesized octahedra were further elucidated by TEM (Figure 3). In agreement with the above FESEM findings, a

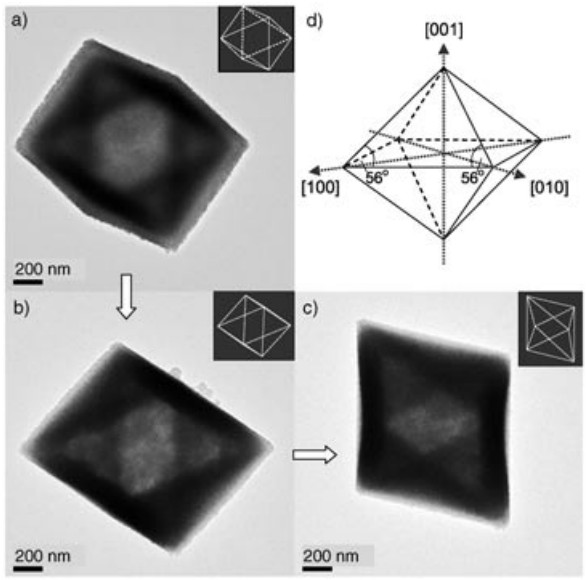

Figure 3. Sequential TEM images (a–c) for a hollow SnO_2 octahedron taken with different tilt angles (a) was viewed perpendicular to the top crystal plane), and a schematic illustration of crystal orientation of an SnO_2 octahedron (d). Edge outlines of the octahedra are depicted in the insets.

high geometric symmetry of the examined octahedron can be seen from the image evolution, while the inner cavity is clearly revealed by the changes in contrast on tilting the sample.

Individual crystal sheets that formed the SnO_2 octahedra can be obtained by sonication (5–10 min in an ultrasonic water bath; Supporting Information). High-resolution TEM (HRTEM; Figure 4a) indicates that triangular SnO_2 sheets are composed of fine crystallites in a size range of only

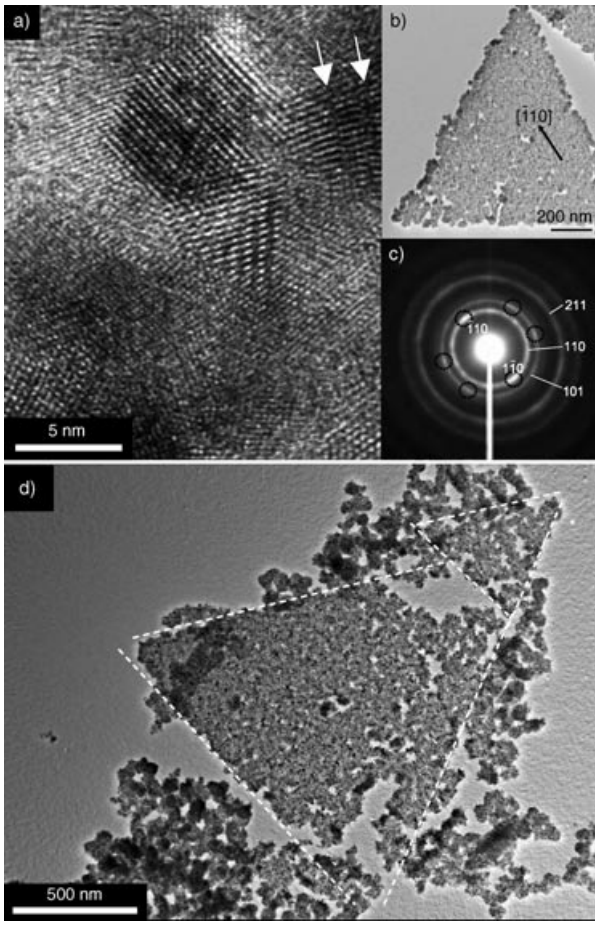

Figure 4. a) Representative HRTEM image of triangular SnO_2 crystallite aggregates (white arrows indicate twin boundaries within a crystallite; spacing $= d_{110}$). b) TEM image of a detached SnO_2 nanocrystalline triangle. c) SAED pattern of the SnO_2 sheet in b). d) Formation of triangles (framed with white dashed lines) from SnO_2 nanocrystallites. Brighter spots (circled) in c) belong to the same set of [111] zone spots.

3–5 nm. These particles were well crystallized, as shown by clear lattice fringes ($d_{110} = 3.3 \pm 0.1$, $d_{101} = 2.6 \pm 0.1$, $d_{200} = 2.4 \pm 0.1$ Å, etc.) and relatively sharp selected-area electron-diffraction (SAED) rings. Although individual crystallites within a local area seem to be random, the overall crystalline aggregates still exhibit global features of {111} vicinal surfaces that suggest long-range ordering of nanocrystallites owing to oriented attachment.[15–19] As can be seen in Figure 4b and c, for example, diffraction spots of (−110) and (1−10) of the [111] zone are visible on the 110 diffraction ring, and they are aligned parallel to the baseline of the triangle, that is, a clear crystalline relationship exists among these [111]-oriented crystallites. Indeed, the lattice fringe of d_{110} is also prominent among the observed nanocrystallites (Figure 4a).

To understand the formation mechanism of the octahedral hollow structures, time-dependent experiments were carried out, which revealed that the hollow octahedra were grown by a plane-by-plane process. As shown in Figure 4d, growth starts with the formation of triangular crystallite aggregates. With appropriate changes in direction at the edges of the triangle (i.e., interplanar angle of 95.2 or 117.1°), further planar coalescence leads to three-dimensional construction of octahedra (Figure 1e and Supporting Information). When two or more such initial sheets are close to each other under low-fluidity conditions, the chance of joining exists (Figure 2a and Figure 4d), that is, the octahedra grow into each other, a process which can be utilized as a means for fabricating even more complex hollow polyhedra. About 5–10% of the octahedra are in this type of joined configuration. It is believed that the addition of ethylenediamine, in combination with the present solvent system, is crucial for stabilizing the {111}-like sheets of SnO_2 while maintaining the small crystallite size. With longer reaction times, smoother crystal facets can be attained for the hollow octahedra, because of continuous surface flattening. Liplike slits arising from accumulated crystal imperfections (twins, disoriented crystallites, etc.), are often found on the edges of the octahedra (e.g., Figure 2c) as a result of mismatched closure. This type of opening may serve as a gateway for materials/chemicals exchange between the interior cavity and exterior space, which is of interest for potential applications of the hollow structures.

In summary, octahedra of rutile-like SnO_2 with a central cavity have been prepared by a template-free hydrothermal route. The synthesis is based on the two-dimensional attachment of nanocrystallites giving an overall {111}-like termination for each octahedral surface in the presence of ethylenediamine and 2-propanol/water. In principle, other hollow polyhedra could also be prepared by stabilizing selected crystal orientations.

Experimental Section

In a typical experiment, SnF_2 (0.24 g) was added to deionized water (50 mL) with vigorous stirring; the pH value was 2.83. The fresh solution (1–2 mL, 0.03 M), deionized water (3–6 g), 2-propanol (13–15 g), and ethylenediamine (1–2 g) were added to a Teflon-lined stainless steel autoclave. The autoclave was kept at 180 °C for 6–50 h in an electric oven. After reaction, white octahedral products were harvested by sedimentation (to separate them from smaller irregular SnO_2 aggregates), washed three times with deionized water, and dried under vacuum overnight. The crystallographic phase of the SnO_2 products was determined by powder XRD (Shimadzu XRD-6000, $Cu_{K\alpha}$ radiation). The products were further investigated by scanning electron microscopy and energy dispersive X-ray spectroscopy (SEM/EDX, JSM-5600LV), field-emission SEM (FESEM/EDX, JSM-6700F), transmission electron microscopy and selected area electron diffraction (TEM/SAED, JEM-2010F, 200 kV), and high-resolution transmission electron microscopy (HRTEM/SAED/EDX, Tecnai-G^2, FEI).

Received: June 30, 2004

Keywords: hydrothermal synthesis · nanostructures · oriented attachment · self-assembly · tin oxide

[1] F. Caruso, R. A. Caruso, H. Möhwald, *Science* **1998**, *282*, 1111.
[2] C. G. Göltner, *Angew. Chem.* **1999**, *111*, 3347; *Angew. Chem. Int. Ed.* **1999**, *38*, 3155.
[3] F. Caruso, *Adv. Mater.* **2001**, *13*, 11.
[4] A. D. Dinsmore, M. F. Hsu, M. G. Nikolaides, M. Marquez, A. R. Bausch, D. A. Weitz, *Science* **2002**, *298*, 1006.

[5] Y. Sun, Y. Xia, *Science* **2002**, *298*, 2176.
[6] Y. Sun, B. Mayers, Y. Xia, *Adv. Mater.* **2003**, *15*, 641.
[7] T. Nakashima, N. Kimizuka, *J. Am. Chem. Soc.* **2003**, *125*, 6386.
[8] C.-W. Guo, Y. Cao, S.-H. Xie, W.-L. Dai, K.-N. Fan, *Chem. Commun.* **2003**, 700.
[9] H. G. Yang, H. C. Zeng, *Angew. Chem.* **2004**, *116*, 5318; *Angew. Chem. Int. Ed.* **2004**, *43*, 5206.
[10] J. Goldberger, R. He, Y. Zhang, S. Lee, H. Yan, H.-J. Choi, P. Yang, *Nature* **2003**, *422*, 599.
[11] B. Liu, H. C. Zeng, *J. Phys. Chem. B* **2004**, *108*, 5867.
[12] H. G. Yang, H. C. Zeng, *J. Phys. Chem. B* **2004**, *108*, 3492.
[13] Y. Yin, R. M. Rioux, C. K. Erdonmez, S. Hughes, G. A. Somorjai, A. P. Alivisatos, *Science* **2004**, *304*, 711.
[14] S. Park, J.-H. Lim, S.-W. Chung, C. A. Mirkin, *Science* **2004**, *303*, 348.
[15] R. L. Penn, J. F. Banfield, *Science* **1998**, *281*, 969.
[16] C. Pacholski, A. Kornowski, H. Weller, *Angew. Chem.* **2002**, *114*, 1234; *Angew. Chem. Int. Ed.* **2002**, *41*, 1188.
[17] X. W. Lou, H. C. Zeng, *J. Am. Chem. Soc.* **2003**, *125*, 2697.
[18] B. Liu, H. C. Zeng, *J. Am. Chem. Soc.* **2003**, *125*, 4430.
[19] B. Liu, H. C. Zeng, *J. Am. Chem. Soc.* **2004**, *126*, 8124.
[20] Z. R. Dai, J. L. Gole, J. D. Stout, Z. L. Wang, *J. Phys. Chem. B* **2002**, *106*, 1274.
[21] Z. R. Dai, Z. W. Pan, Z. L. Wang, *J. Am. Chem. Soc.* **2002**, *124*, 8673.
[22] Theoretical values are 54.1 and 71.8°, respectively; the observed deviation is probably due to the presence of disoriented crystallites and crystal defects in the triangular sheets that result in mismatched planes.

